INFLUENCE OF THE SIGNAL COIL ON DC-SQUID DYNAMICS

Heikki Seppä
Electrical Engineering Laboratory, Technical Research Centre of Finland
Otakaari 7B SF-02150 ESPOO, Finland
and
Tapani Ryhänen
Dept. of Electrical Engineering, Helsinki University of Technology
Otakaari 5A SF-02150 ESPOO, Finland

Abstract – The dynamics of the dc-SQUID in the presence of a signal coil was studied. The signal coil creates an additive parasitic capacitance between the junctions and its self-resonance imports new features to the SQUID dynamics. Our results suggest that if a SQUID with smooth characteristics and low noise properties is desired, all the resonances present in the SQUID ring or in the flux coupling circuit should be damped properly. Low attenuation yields a system with high gain but with higher excess noise. On the other hand, heavy damping of the device yields low gain and a high noise level and thus a compromise is necessary.

I. INTRODUCTION

The improvement of SQUID magnetometers is mainly achieved by improving the efficiency of the magnetic coupling. Most of the systematic studies carried out thus far have been with automous SQUIDs, sometimes even with ignoring the junction capacitances. Simple models may be applicable also with high β_c devices but major problems will arise determining the characteristics of strongly coupled SQUID magnetometers. Slightly better agreement between theoretical and practical devices is achieved by including junction capacitances. Unfortunately, these analyses have led to the false impression that high values for the parameters β and β_c can be a basis for the successful SQUID design. The presence of parasitic elements, unwanted companions of the signal coil, may change the SQUID dynamics sufficiently to cancel the design criteria estimated with the aid of autonomous SQUIDs. External effects associated with the flux coupling circuit include at least the following: the $\lambda/2$-resonances in transmission lines produced by the SQUID loop and the signal coil, the self resonance of the flux transformer and the parasitic capacitance shunting of the SQUID loop.

The principal aim of this work was to analyse the dynamics of the SQUID including the flux transforming circuit. The simulations were carried out with a digital computer using a Taylor-expansion routine /1/. Since in addition to extra circuits, thermal noise sources generated by shunt resistors are also modeled, some of the numerical simulations became very massive. Consequently, no real optimizations could be performed. The simulations were carried out to gain better insight into the characteristics of the SQUID dynamics and to promote work aimed at systematizing practical SQUID design.

The computer simulations were performed using three different models for the dc-SQUID: in the first model the junctions are described by the RSJ model with finite junction capacitances. This simple model is treated here only to compare the results with those discussed in literature. Secondly, the stray capacitance introduced by the signal coil is included and the characteristics are investigated by varying both the junction and the parasitic capacitances. The most laborious simulations are carried out by modeling the flux transformer, including the stray capacitance of the input coil and an additive lossy capacitance. The circuit model can be used to study SQUID magnetometers having an open or an inductively shunted signal coil.

Manuscript received September 30, 1986

II. SQUID CIRCUIT MODEL

The most complex circuit model for the dc-SQUID magnetometer used in the simulations is depicted in Fig. 1. Josephson elements are described by a critical current I_0, a shunt resistor R and a junction capacitance C. The junctions are connected together through the inductance L disturbed by a parasitic capacitance C_P. The signal coil is described by an inductance L_S and a parallel capacitance C_S. An external capacitance C_X with resistance R_X in series is inserted to the flux transformer to damp the Q-value of the resonating input coil. We chosen not to use any resistor crossing the signal coil since this would introduce additional thermal noise at low frequencies. The coupling coefficient α is defined by means of the mutual inductance M as $\alpha=M/\sqrt{L_S L}$. The inductance L_{ext} drawn with the dashed line describes a pick-up coil commonly used in a practical device. Actually, this inductance is in parallel with L_S and therefore can be quantizied simply by offseting the values of the other circuit parameters. In Fig. 1 the finite temperature is described by two current sources in parallel with the junctions.

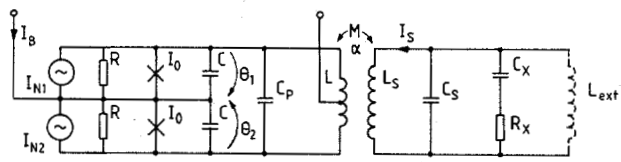

Fig. 1. Schematic diagram of a dc-SQUID with a flux coupling circuit.

Following the equivalent circuit shown in Fig. 1, the dynamics of the device can be shown to be governed by the set of dimensionless equations

$$\beta_c\ddot{\vartheta} + \dot{\vartheta} + \sin\vartheta\cos\varphi = i + i_{N1} \tag{1}$$

$$\beta_k\ddot{\varphi} + \dot{\varphi} + \sin\varphi\cos\vartheta + 2(\varphi-\pi\varphi_A)/\beta = -2\alpha^2 i_s + i_{N2} \tag{2}$$

$$\beta_s\beta_x\beta_t\dddot{i}_s + \beta_s\beta_t(1+\wp_c)\ddot{i}_s + \beta_x\dot{i}_s + i_s = \beta_x\beta_s\dddot{\varphi} + \beta_s(1+\wp_c)\ddot{\varphi} \tag{3}$$

where

$$\beta=\frac{2LI_0}{\Phi_0},\ \beta_c=\frac{2\pi R^2 I_0 C}{\Phi_0},\ \beta_k=(1+2\frac{C_P}{C})\beta_c,\ \beta_s=\frac{C_S}{C}\beta_c,\ \wp_c=\frac{C_X}{C_S}$$

$$\beta_x=\frac{C_X R_X}{CR}\beta_c,\ \beta_t=(1-\alpha^2)\beta,\ i=\frac{I}{2I_0},\ i_s=\frac{I_S}{2\alpha I_0},\ i_{Ni}=\frac{I_{Ni}}{2I_0}$$

$$\varphi_A=\frac{\Phi_A}{\Phi_0},\ S_{i_{N1}}(\omega)=S_{i_{N2}}(\omega)=\frac{\Phi_0}{\pi RI_0}\Gamma,\ \Gamma=\frac{2\pi k_B T}{I_0\Phi_0}$$

Here the overdots denote derivatives with respect to the dimensionless time given in the commonly used units $\Phi_0/(2\pi I_0 R)$. Φ_A is the external flux applied to the SQUID loop. ϑ and φ describe the average phase, $(\phi_1+\phi_2)/2$, and the difference of phases, $(\phi_1-\phi_2)/2$, with ϕ_i denoting the quantum phase difference across

0018-9464/87/0300-1083$01.00©1987 IEEE

the ith junction. As mentioned above we inspected the dynamics of the SQUID with the three different models for the device. The simplest model was obtained from Eqs. (1) and (2) by setting $\beta_c=\beta_K$ and $\alpha=0$. When modeling the appearance of the signal coil only with a parasitic capacitance, α will remain zero but $\beta_c\neq\beta_K$. The influence of the signal coil is obtained more precisely by running the whole set of the equations. The noise from the lossy elements in the signal coil is deliberately ignored.

III. NUMERICAL SIMULATION

As was mentioned above the simulations were made by a digital computer using a Taylor expansion method. The time interval required by the average phase to pass the distance of 2π was stored. The average velocity and the power spectrum were then computed after resampling the stored data. An FFT-routine was applied to determine the voltage spectrum and the flux noise was defined from its low frequency limit. The remainder of this paper is devoted to discussing separately the SQUID characteristics introduced by the different circuit models.

A. *DC-SQUID without a signal coil*

De Waal et.al. have computed the performance of a SQUID with a finite junction capacitance using an analog computer /2/. Their simulations indicated that the optimum energy resolution was $\epsilon\cong\beta\Gamma$ (in dimensionless units), even if both β and β_c were allowed to vary between 1 and 2. The results seemed to suggest that even higher values for β-parameters may be a foundation for instrument design. High values of the parameters undoubtedly introduce some instability to the system and thus excess noise will inevitably be incorporated. Fortunately two simultanous effects moderate the influence of the excess noise on the energy sensitivity: the transfer gain $\partial V/\partial\Phi_A$ increases and down-mixed noise decreases with increasing β-parameters. We studied the

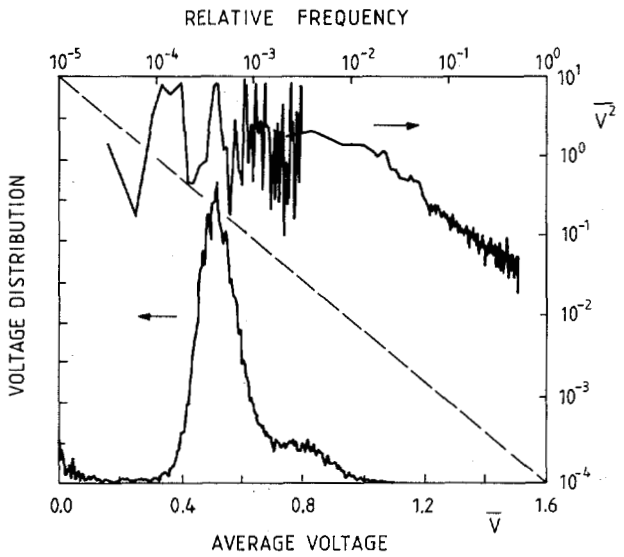

Fig. 2. Upper right hand corner: Voltage noise power spectral density of the SQUID with $i=0.9$, $\beta=2$, $\beta_c=3$, $\Gamma=0.05$, and without the external flux. Lower left hand corner: Probability distribution of the voltage according to the data used for the voltage noise spectrum.

performance of an autonomous SQUID with up to 3 β-parameters. Our results agreed well with those given by de Waal et.al /2/ and on the other hand by D. Drung and W. Jutzi /3/. As a demonstration one of our results obtained from the SQUID with $\beta=2$, $\beta_c=3$, $\Gamma=0.02$ is illustrated in Fig. 2. Excursions at the static state, the beating state and the running state can clearly be seen from the voltage distribution drawn in the inset figure. The voltage spectrum increases towards low frequencies by two powers of ten with a 1/f-dependence, confirming the simultaneous excitence of several states. At this specific point of operation transitions between the different states produce additive noise by factor of hundred. Some similar results will be published elsewhere /4/.

B. *DC-SQUID with a parasitic capacitance*

The increasing parasitic capacitance reduces the damping in eq. 2 and consequently invigorates beating-type motions in the SQUID dynamics. Most of our simulations was performed to test the hypothesis that if the ratio C_P/C is much less than unity the dynamics of the SQUID will remain unchanged at the practical operation points. In other words we argue that the dc-SQUID with junction capacitance C and stray capacitance C_P provides nearly the same resolution as the device with junction capacitance $C+2C_P$. Moreover, the practical SQUID can be dimensioned with the aid of conventional knowledge. The I-V characteristics of the two devices with identical inductances and critical currents are shown in Fig. 3. One is assumed to suffer from the parasitic capacitance while the other does not. As the curves indicate no great difference in voltage arises if the bias flux differs from zero and if the points of operation do not exceed the loop resonance. The general insight arising from the simulations was that the SQUID with small stray capacitance and with finite external flux functions in the same manner as other SQUIDs having an equivalent self-resonance. Zero flux does not necessarily generate a current to flow between the junctions and thus the parasitic capacitance remains insignificant.

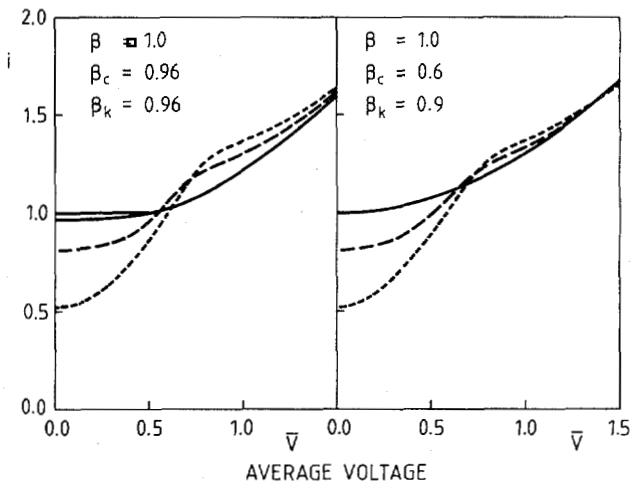

Fig. 3. Current-voltage characteristics of the SQUID with $\beta_c=\beta_K=0.96$ (left hand side) and of the device with $\beta_K=0.6$ and $\beta_c=0.9$ (right hand side). The both characteristics are obtained with $\beta=1$ and without external flux (solid lines), 1/4 (dashed lines), and 1/2 (broken lines).

If the stray capacitance is allowed to exceed the junction capacitance excess noise will dramatically increase and even worse, the flux sensitivity will be lost. Fig.4 shows the I-V-curve of the SQUID with $C_P/C=31.52$, $\beta=1$, and $\beta=0.7$. Open circles, filled circles and squares indicate the voltage at different external fluxes. The data points touch each other, indicating the poor gain of the device. If there is no

thermal noise to activate transitions between multiple modes, srongly hysteretic I-V characteristics will result. At very high values of β_c the dominant feature is the appearance of a staircase type I-V characteristic as demonstrated and discussed by D. Drung and W Jutzi /5/. If practical considerations compel the acceptance of a high stray capacitance it is undoubtedly profitable to attenuate the SQUID loop as recomended by Enpuku et.al. /6/ and M. Gershenson et.al. /7/.

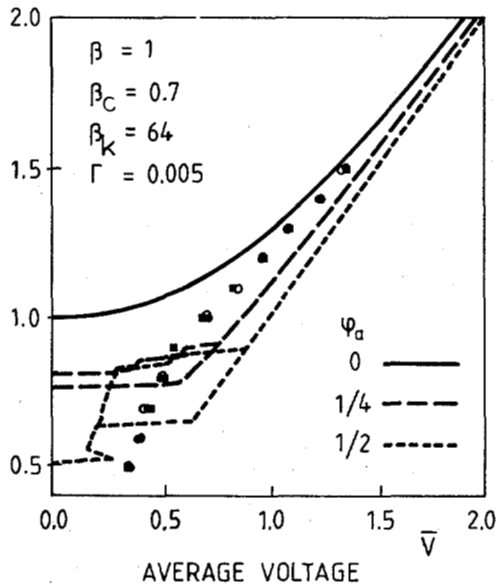

Fig. 4. i-v-curves of a SQUID with high parasitic capacitance. Different lines illustrate the characteristics in the absence of thermal noise while circles and squares in the presence of thermal noise.

C. *SQUID with a lossy signal coil*

The main result of this work is the demonstration of the importance of damping all resonances appearing at any frequency. We would also like to show that the resonances, locating at much lower frequencies than the average frequency of operation, could be disastrous. The endless aim of maximizing the gain of the device drives undeniably the operation point at the place from which the frequent exursions at the zero voltage state will occur. If any resonance appears on the way to the static state the system will no doubt trap there. The time which the system spends in the trap is proportional to the resonant frequency multiplied by the Q-value. Avoiding excess noise by seating the system at high voltage generates a system with modest gain, only heavily damped SQUIDs produce some gain at high voltages. It should be emphasized here that the simulations which ignored junction capacitances may give a completely incorrect impression of the characteristic of the SQUID affected by the signal coil resonance: the signal coil resonance can also be attenuated by shunt resistors intended originally for the junctions; the gain is also available at high voltage levels; the SQUID undisturbed by the signal coil is not sensitive to drift to the zero voltage state. In other words if the large capacitance junctions are intended to be utilized the resonances in the flux coupling circuits should be considered seriously.

We have investigated the performance of a SQUID while damping the signal coil by varying the resistance R_x. Other parameters are appropriate for a typical dc-SQUID. The simulation results have been collected into Fig. 5. The set of smooth curves in the upper left corner, Fig. 5 (a), shows the noiseless voltage vs. current characteristics of the SQUID in the absence of the signal coil. Similar curves are also obtained in the presence of the signal coil. Since the thermal noise does not activate frequent excursions to the static state, the resonance remains invisible to the SQUID dynamics and if the point of operation is chosen away from the resonance the results are equivalent to an autonomous SQUID. The next three sets of curves are

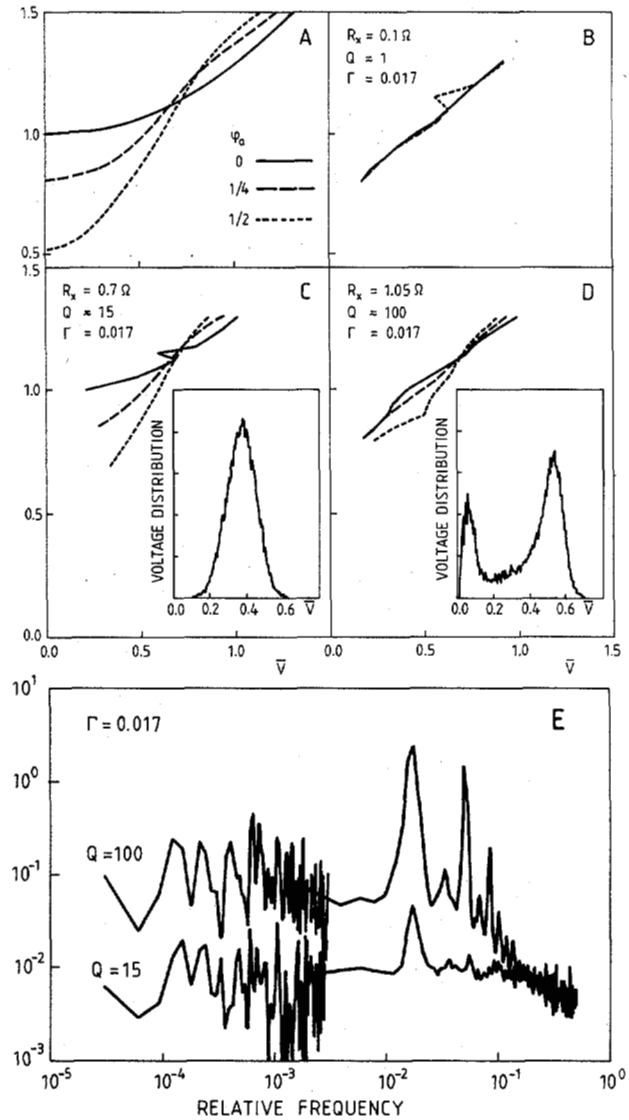

Fig. 5. Current voltage characteristics of the SQUID at different values for the damping resistace R_x. The inset figures (C,D) show the corresponding voltage distriutions. The curves in the upper left hand corner (A) illustrate the i-v-characteristics of the SQUID without the flux coupling circuit. (E) Voltage noise power spectral density of the SQUID with two different Q-values of the signal coil. The simulations were carried out with the following values for the parameters: C=1pF, C_S=10pF, C_X=100pF, C_P=0.15pF, L=0.1nH, L_S=10nH, I_o= 10.3μA, R=4.7Ω, and T=4.2K.

found in the presence of thermal noise. The difference is dramatic: noise has introduced transitions between the multiple solutions, thus revealing the resonance which was hidden between the static and the beating states. As the figures depict, the flux to voltage efficiency is strongly reduced. The best result is clearly that carrying the label R=0.7Ω and Q=15. High damping ruins the gain of the system, while negligible

damping does not prevent the system from hopping between different states. In order to provide further light on the resonance effect the corresponding voltage distributions are given in Figs. 5 (c) and 5 (d) and the voltage power spectrums in Fig. 5 (e). As the inset figures illustrate, the higher the value of Q the longer is the time which the system spends in the resonant state. According to Fig. 5 (e) the high Q-device seems to produce ten times higher voltage noise compared with that having the Q-value of 15. It is also evident that the system may be locked temporarily on some harmonics of the resonant frequency.

All the simulations were carried out by fixing the coupling coefficient α at the value of 0.025. This low value may sound curious since in a state-of-the art SQUID α may increase almost 0.95. Our low value can be defended as follows: the primary model does not include the pick-up coil but it can be included by offseting the values of the original parameters. Secondly, the total length of the signal coil is usually several wavelengths of the Josephson oscillation at the average point of operation, thus reducing effectively the coupling constant. At low frequencies the signal coil acts as a lumped element having strong coupling to the SQUID loop. Consequently, while residing at high voltage states the SQUID receives no input concerning the presence of the signal coil. At the moment thermal noise activates the system to lower voltage states the resonance will be revealed by the magnetic coupling. Unfortunately, this feature is too complex to be modeled. We believe, however, that the frequency independent α-parameter will remain the main features of the practical device. Evidently, the drawback of the inexact model is that we are unable to give any precise instructions for dimensioning the device.

The energy sensitivity best describes the performance of the dc-SQUID magnetometer. With this in mind the gain of the system was also evaluated at the flux bias point $\varphi_A=1/4$ and the bias current producing the best possible performance was chosen. The high damping tends to push the bias current to low values, the resonance with low Q being less actractive than the that with high Q. A SQUID with the same parameters as those given in Fig. 5 has the following energy sensitivities: $\epsilon\cong 400\beta\Gamma$ (R=0.1Ω, i=0.95), $\epsilon\cong\beta\Gamma$ (R=0.7, i=0.9), $\epsilon\cong 10\Gamma\beta$ (R=1.1, i=0.9). The most important observation here is that proper attenuation may lead to a magnetometer with a resolution comparable with that attained with an optimized autonomous SQUID (see Ref. 2). It should emphasized here that thermal noise from R_x is ignored and the resonance locating at a very low frequency may reduce the resolution of the device.

The dependence of the excess noise on the system parameters may be approximately estimated as follows: Since the resonance is not visible to the system operating at high voltage states the probability that the system will cross the resonance on its way to the static state depends only on the paramters of the autonomous SQUID. The mean lifetimes of different states can evaluated by numerical methods or by applying the theory presented by Ben-Jacob et. al. /8/. If the average lifetime of the resonant state is assumed to be the quality factor multiplied by the resonant frequency the total time which the system spends in the resonance trap can be approximated. No doubt the additive noise depends strongly on the operation point and is inversely proportional to the damping resistance R_X. In a practical device the bias current is optimized, thus making the system much more insensitive to the lossy factor of the shunt capacitor C_x.

As was mentioned above our model is extremely massive and thus practical SQUID dimensioning cannot be based on these results. Therefore the proper attenuation of the signal coil must be determined experimentally. This kind of work is recently being carried out and the preliminar results are in a good agreement with those qualitively predicted in this work /9/.

IV CONCLUSION

The purpose of this paper was to outline the importance of the signal coil to the performance of SQUID magnetometers. In particular we wish to emphasize the fact that many features of the dynamics remain undetected if the circuit model is imperfect. Of course the presence of the signal coil inroduces many unwanted effects and it is impossible to include them all.

The problems associated with the flux coupling circuits should be taken seriously and the dimensioning of the SQUID must be realized accordingly. On the basis of the simulations we may propose the following approach for the SQUID design: the actual SQUID ring should be small in order to avoid the first $\lambda/2$-resonance; the coupling circuit should not be allowed to create a parasitic capacitance higher than that caused by the junctions. The length of the signal coil should be sufficient to reduce the effective coupling at high frequencies. Both the transmission-type and the LC-type resonances related with the presence of the signal coil should be properly damped. β_c and β should not exceed unity in order to suppress transitions between the multiple solutions. This kind of approach favours a SQUID with a low loop inductance and a magnetic coupling composed of two transformers connected in series /10/. Tesche has shown that low noise magnetometers can also be produced without damping the resonant circuits /10/. This kind of approach is profitable only if the junctions with extremely low capacitance are available. The well-damped SQUIDs also held the promise of reduced 1/f-noise /11/.

ACKNOWLEDGEMENT

We would like to thank Juhani Kurkijärvi and Jukka Ketoja of the Department of Technical Physics, Helsinki University of Technology, Jukka Knuutila and Antti Ahonen of the Low Temperature Laboratory and Jorma Salmi and Risto Mutikainen of the Semiconductor Laboratory, VTT (Technical Research Centre of Finland) for valuable discussions during the work. We also express our gratitude to Pekka Wallin and Toivo Katila, Helsinkin University of Technology, for their support to the project.

REFERENCES

1. J.A.Ketoja, J.Kurkijärvi,and R.K.Ritala, Phys.Rev. B30, 3757 (1984)
2. V.J. de Waal, P.Schrijner, and R.Llurba, J.Low Temp.Phys.54, 215 (1984)
3. D.Drung and W.Jutzi, IEEE Trans.Magn. MAG-21, 430 (1985)
4. J.A.Ketoja, J.Kurkijärvi, T.Ryhänen, and H.Seppä, Phys.Rev.B (submitted to be published)
5. D.Drung and W.Jutzi, in Superconducting Quantum Interference Devices and Their Applications, edited by H.D.Hahlbohm and H.Lubbig (de Gruyter, Berlin, 1985), p.807
6. K.Enpuku, K.Sueoka, and K.Yoshida, J.Appl.Phys.57, 1691 (1985)
7. M. Gershenson, R. Hastings, R. Schneider, M. Sweeny, and E. Sorensen, IEEE Trans.Magn. MAG-19, 2058 (1983)
8. E.Ben-Jacob, D.J.Bergman, Y.Imry, B.J.Matkowsky, and Z.Schuss, J.Appl.Phys.54, 6533 (1983)
9. The measurements were carried out at the Low Temperature Laboratory using the SQUIDs from IBM, the results will be published later on
10. C.D.Tesche, J.Low Temp.Phys.47, 385 (1982)
11. H.Seppä, T.Ryhänen, and J.Kurkijärvi, Phys.Rev.B (submitted to be published)